

# Empowering LLMs to Understand and Generate Complex Vector Graphics

Ximing Xing, Juncheng Hu, Guotao Liang, Jing Zhang  
Beihang University

{ximingxing, hujuncheng, 1780760951, zhang\_jing}@buaa.edu.cn

Dong Xu  
The University of Hong Kong  
dongxu@cs.hku.hk

Qian Yu\*  
Beihang University  
qianyu@buaa.edu.cn

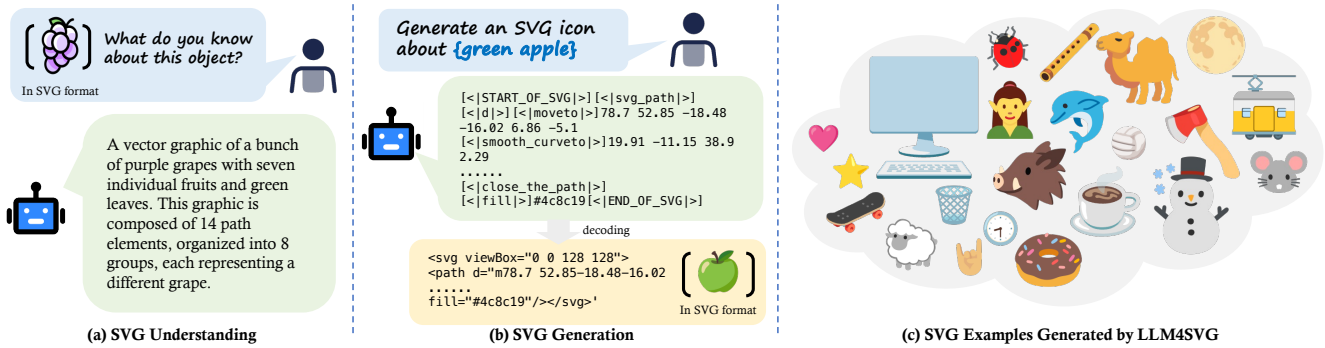


Figure 1. **Our LLM4SVG can understand and generate vector graphics from textual description.** Our LLM4SVG is designed to: (a) Understand the semantics of SVG (Scalable Vector Graphics) source code and directly extract the meanings conveyed by vector images; (b) Generate corresponding structured SVG representations from textual prompts and decode them into SVG source code that accurately reflects the described content. (c) illustrates some SVG examples generated by our method.

## Abstract

The unprecedented advancements in Large Language Models (LLMs) have profoundly impacted natural language processing but have yet to fully embrace the realm of scalable vector graphics (SVG) generation. While LLMs encode partial knowledge of SVG data from web pages during training, recent findings suggest that semantically ambiguous and tokenized representations within LLMs may result in hallucinations in vector primitive predictions. Additionally, LLM training typically lacks modeling and understanding of the rendering sequence of vector paths, which can lead to occlusion between output vector primitives. In this paper, we present LLM4SVG, an initial yet substantial step toward bridging this gap by enabling LLMs to better understand and generate vector graphics. LLM4SVG facilitates a deeper understanding of SVG components through learnable semantic tokens, which precisely encode these tokens and their corresponding properties to generate semantically aligned SVG outputs. Using a series of learnable semantic tokens, a structured dataset for instruction

following is developed to support comprehension and generation across two primary tasks. Our method introduces a modular architecture to existing large language models, integrating semantic tags, vector instruction encoders, fine-tuned commands, and powerful LLMs to tightly combine geometric, appearance, and language information. To overcome the scarcity of SVG-text instruction data, we developed an automated data generation pipeline that collected a massive dataset of more than 250k SVG data and 580k SVG-text instructions, which facilitated the adoption of the two-stage training strategy popular in LLM development. By exploring various training strategies, we developed LLM4SVG, which significantly moves beyond optimized rendering-based approaches and language-model-based baselines to achieve remarkable results in human evaluation tasks. Code, model, and data will be released at: <https://ximinng.github.io/LLM4SVGProject/>

## 1. Introduction

Scalable Vector Graphics (SVGs) represent a fundamental method of image encoding, where visual elements are

\*Corresponding author.

formed from basic shapes like vector paths, curves, and polygons, defined by mathematical equations. This contrasts with raster graphics, which depict images as pixel arrays on a grid. One of the key advantages of vector graphics is their capacity to preserve high precision and consistent visual quality across varying resolutions, as they can be scaled indefinitely without any loss of detail. Additionally, vector graphics typically maintain compact file sizes, which enhances their efficiency for storage and transmission. More critically, they offer superior editability, enabling designers to easily select, modify, and compose elements. This attribute is particularly vital during the design process, facilitating seamless adjustments and fostering creative exploration. Due to their inherent properties, SVGs are particularly well-suited for applications in visually fluent design.

In recent years, there has been a significant increase in interest in vector graphics generation [11, 20, 23, 33, 43, 53, 58, 66, 67, 73]. Notwithstanding the significant advantages inherent to SVGs, current deep learning-based generative methods still face limitations in producing high-quality, complex SVG outputs. The current approaches [4, 16, 29, 41, 51, 61, 63] represent SVGs using a restricted command path and leverages sequential model learning. Such methods predominantly engage with simplified SVGs, confined to basic path commands (*e.g.* move to, line to, cubic bézier) and are frequently limited in complexity; certain approaches focus exclusively on fundamental fonts [29] or icons [61]. Recent innovations [23, 53, 66, 67, 73] have incorporated advanced image diffusion models [38, 44] to facilitate the generation of raster images, subsequently translated into SVG format via a differentiable rasterizer [27] predicated on Bézier curve representations. While the utilization of generative raster images introduces a degree of variety, this process is characterized by an cumbersome iterative procedure, and the resultant SVGs remain non-editable and fail to align with the expectations of professional designers. In light of these developments, a critical gap persists in the realm of systems capable of directly synthesizing intricate and detailed SVG code, fully leveraging the comprehensive array of SVG primitives requisite for sophisticated design applications.

Recent advancements in large language models (LLMs) [2, 28, 34, 39, 55] have evidenced their capacity to comprehend and parse XML syntax [5], achieved through extensive pre-training on a diverse corpus of text data sourced from the Web. This proficiency establishes a robust foundation for LLMs to synthesize vector graphics [43]. Notably, state-of-the-art models, such as ChatGPT [34] and GPT-4 [2], show proficiency in generating simple vector primitives like triangles and rectangles; however, they often encounter significant limitations in synthesizing complex graphics. This is because, during pre-training, SVG data from the Internet is often embedded within web page code,

requiring LLMs to parse layered languages, which renders SVG data less accessible amidst lengthy XML tags. These limitations manifest as confusion or hallucinations in vector path sequences, yielding semantically ambiguous graphics and improperly encoded attributes.

In this paper, we present LLM4SVG, an initial yet substantial step toward bridging this gap by enabling LLMs to better understand and generate vector graphics, as illustrated in Fig. 1. Built on an existing LLM, such as GPT-2 [39] and LLaVA [28], LLM4SVG maximizes the model’s potential for vector graphic synthesis. Our paper makes the following contributions:

- **Introducing LLM4SVG: Advancing LLM Capabilities for SVG Understanding and Generation.** We present LLM4SVG, a pioneering model designed to bridge the gap in SVG generation within large language models (LLMs), addressing challenges in accurately predicting vector primitives and managing occlusions. By utilizing learnable semantic tokens, LLM4SVG enables LLMs to effectively encode SVG components and properties, aligning generation outputs with human design standards and reducing the risk of semantic ambiguities.
- **Modular Architecture Integrating Geometric, Visual, and Linguistic Features.** LLM4SVG features a modular design that augments traditional LLM architectures with a vector instruction encoder, semantic token embedding, and regression heads for precise coordinate and color predictions. This multimodal integration facilitates a comprehensive understanding of SVG elements, enabling LLMs to generate refined, semantically consistent vector graphics by effectively merging geometry, appearance, and linguistic information.
- **Development of a Large-Scale SVG-Text Dataset and a Two-Stage Training Strategy.** Addressing the lack of SVG-Text instruction data, LLM4SVG introduces an automated pipeline that collects 580k SVG-text instruction pairs. We collected 250k SVG samples designed by human designers. This large-scale dataset supports a two-stage training strategy, which enhances LLM comprehension and performance in SVG generation tasks, setting a robust foundation for further advancements in SVG-related capabilities within LLMs.

## 2. Related Work

### 2.1. Vector Graphics Synthesis

Scalable Vector Graphics (SVGs) provide a declarative format for visual concepts articulated through primitives. One approach to generating SVG content entails training a neural network to generate predefined SVG commands and attributes [4, 16, 29, 41, 51, 61, 63]. Neural networks designed for learning SVG representations typically include architectures such as RNNs [16, 41], VAEs [4, 29, 51], and

Transformers [4, 61, 63]. The training of these networks is heavily dependent on datasets in vector form. However, the limited availability of large-scale vector datasets significantly constrains their generalization capability and their ability to synthesize intricate vector graphics.

Li *et al.* [27] introduce a differentiable rasterizer that bridges the vector graphics and raster image domains. While image generation methods that traditionally operate over vector graphics require a vector-based dataset, this approach for SVG generation [20, 30, 47–49, 54] involves directly optimizing the geometric and color parameters of SVG paths using the guidance of a pretrained vision-language model. Recent advances in visual text embedding contrastive language-image pre-training model (CLIP) [40] has enabled a number of successful methods [11, 33, 58] for synthesizing sketches. In contrast to CLIP, several methods [23, 66, 67] integrate diffusion models with differentiable rasterizers to achieve superior generation capabilities and enhanced image consistency. Moreover, recent studies [53, 73] combine optimization-based approaches with neural networks to learn vector representations, incorporating geometric constraints into vector graphics.

## 2.2. Large Language Models

Large Language Models (LLMs) have achieved substantial progress in natural language understanding, exhibiting strong generalization and reasoning capabilities to complete real-world applications through extensive pre-training on large-scale textual datasets, such as ChatGPT [34]/GPT-4 [2], LLaMA [55], Claude 3.5 [35], Qwen 2.5 [52], Gemini [7], Grok-2 [65], Yi [70], Falcon [3], Phi series [1, 24, 32], etc.

Broadly, LLMs can be classified into two categories. The first category includes models that employ a large language model to interface with individual, modality-specific models [15, 21, 37]. This approach circumvents the need for model training but is heavily dependent on the availability and capabilities of pre-existing models or APIs. The second category includes models that use an end-to-end training strategy, comprising two main paradigms. The first involves training the model from scratch, similar to text-only LLMs, using large-scale multi-modal corpora and datasets [2, 22]. Instead of training an LLM from scratch, it is more efficient and practical to start with a pre-trained one [28]. In our work, we adopt a fine-tuning strategy based on pre-trained LLMs, focusing on adapting the model to generate and understand vector graphics. While multi-modal capabilities can be incorporated when needed, our primary emphasis is on leveraging the pre-trained LLM’s robust foundational knowledge and generalization abilities, which provide a strong basis for specialized, task-oriented applications in the vector graphics domain.

The adaptability of LLMs also extends naturally into

the multi-modal domain. This has enabled them to be utilized not only for text-based tasks but also as foundational architectures for expanding into multi-modal applications. Building on this foundation, Multi-modal Large Language Models (MLLMs) are designed to interpret and generate content across various modalities, including but not limited to images [13, 22, 28, 59, 60, 74], audio [8, 21], motion [25, 72], and 3D point clouds [18, 68].

## 2.3. Instruction Tuning

In the field of natural language processing (NLP), researchers have investigated various methods [34, 36, 62] for instruction-tuning LLMs, aiming to enhance their ability to follow natural language instructions and perform real-world tasks. It has been found that this simple and straightforward approach can significantly enhance the zero-shot and few-shot generalization capabilities of LLMs. With the growing popularity of multimodal large language models (MLLMs), LLaVA [28] has utilized visual instruction tuning with vision-language instruction data, significantly enhancing the performance of open-source MLLMs on multi-modal tasks.

Recently, several studies have explored directly fine-tuning LLMs with image embeddings for generating Scalable Vector Graphics (SVG) by treating SVG code as a text-based representation [43, 69]. While these methods have shown promise in applying LLMs to vector graphics generation, they often overlook the hierarchical and structured nature of SVG files, treating them as sequential text. Additionally, most LLMs [1, 52, 59] often treat numbers as individual characters, making it difficult for them to understand continuous numerical data, such as coordinates. This simplification can restrict the model’s ability to fully capture the SVG’s complex dependencies and file structure, which can impact the quality and semantic accuracy of the generated graphics.

## 3. Vector Instruction Following Data

A significant obstacle in developing an end-to-end LLM is the acquisition of large-scale instruction-following data, which is indispensable for representation learning, aligning latent spaces, and guiding models to align with human intent [28]. In the domain of vector graphics, this obstacle is particularly acute, as the high production cost and tagging challenges associated with vector graphics constrain current research to a limited scope of applications. These areas include simple human hand drawings [45, 71], fonts [29], and iconic graphics [4, 6].

To address these challenges, we manually collected approximately 250,000 colorful and complex vector graphics and developed a normalization process to ensure that the collected data conformed to a consistent standard, including uniform canvas size, relative coordinate systems, and repre-

Type	Role	Content Template
# 1	SYSTEM	You are a helpful assistant, please help me generate SVG </s>
	USER	Generate an SVG based on the following text: {prompt} </s>
	ASSISTANT	SOV Path MoveTo Coord LineTo Coord ... FILL RGB ... EOV </s>
# 2	SYSTEM	You are a helpful assistant, please help me generate SVG by referring to this image </s>
	USER	Refer to this image: {img} and generate SVG based on the following text: {prompt} </s>
	ASSISTANT	SOV Path MoveTo Coord LineTo Coord ... FILL RGB ... EOV </s>
# 3	SYSTEM	Attempt to identify this SVG </s>
	USER	The following is an SVG illustration: SOV Path <sub>1</sub> ... Path <sub>n</sub> EOV
	ASSISTANT	Text description of this SVG: {desc} </s>
# 4	SYSTEM	Attempt to understand the path composition in this svg </s>
	USER	The following is an SVG illustration: SOV Path <sub>1</sub> ... Path <sub>n</sub> EOV rendering result: {img}
	ASSISTANT	Text description of this SVG: {desc}. This SVG contains {n_path} primitives. </s>
# 5	SYSTEM	Attempt to understand the path composition in this svg </s>
	USER	SVG path group 1: GROUP Path <sub>1</sub> ... Path <sub>3</sub> EOG rendering result: {img} <sub>1</sub>
	USER	SVG path group 2: GROUP Path <sub>6</sub> ... Path <sub>9</sub> EOG rendering result: {img} <sub>2</sub> </s>
	USER	Text description of this SVG: {desc}
	ASSISTANT	The 1st SVG group contains {n_paths} <sub>1</sub> primitives representing {desc} <sub>1</sub> The 2nd SVG group contains {n_paths} <sub>2</sub> primitives representing {desc} <sub>2</sub> </s>

Table 1. **Instruction Following Template.** We developed five distinct instruction templates tailored for tasks in vector graphics generation and understanding. Specifically, Types #1 and #2 facilitate the generation task, while Types #3, #4, and #5 focus on the understanding task. {prompt} denotes a brief image caption generated via BLIP [26], {n\_paths}<sub>i</sub> represents the total number of primitives in group *i*, {desc} provides a detailed GPT-4 [2] generated description, and Token represents different types of SVG semantic tokens. Path<sub>i</sub> serves as the representation of a complete SVG primitive, encompassing a structured set of SVG semantic tokens essential for comprehensive vector graphic description. Types #1~#5 provide a structured framework for training SVG semantic tokens, facilitating more accurate vector representation and understanding. Losses are computed only on model responses. </s> indicates the end-of-sentence token. “SYSTEM” is an instruction that describes the type of task, specifically the context of the conversation. “ASSISTANT” denotes the output generated in response to the instruction, representing the LLM’s reply. “USER” refers to the input data provided by the user.

sentation. These high-quality vector datasets provided us with a solid foundation for the development of LLM4SVG. Additionally, inspired by the recent success of GPT models in text annotation tasks [12], we utilized BLIP [26] to annotate rasterized vector graphs and GPT-4 [2] for instruction-following data collection.

**SVG Re-captioning.** SVG data collected from the Internet often contains noise, and directly using it for learning can compromise the model’s potential representational accuracy. Approximately half of the data in an SVG file is redundant for visual rendering. This redundancy includes: (1) temporary data used by vector editing applications, (2) non-optimal structural representations of SVG, and (3) unused and invisible graphic elements. We propose an SVG data preprocessing pipeline designed to losslessly reduce the size of SVG files generated by vector editing applications. Details are provided in Sec. B and Fig. S5 of Supplementary. This pipeline incorporates a combination of carefully optimized strategies that address four key aspects of SVG files: elements, attributes, paths, and outputs. After optimizing the SVG, we rasterize it into an image of  $512 \times 512$  pixels and use the BLIP [26] model to generate a corresponding caption as a text prompt. Consequently, we obtain a multimodal dataset, each entry of which is a triplet consisting of the optimized SVG, its corresponding raster-

ized image, and a text description generated by the BLIP model.

Subsequently, we propose a strategy for the automatic generation of SVG instruction-following data. As outlined in Table 1, the instruction data are categorized into two distinct parts: the first (items #1 and #2) addresses the synthesis of vector graphics, while the second part (items #3, #4, #5) pertains to the comprehension of vector graphics.

**SVG Instruction Data.** The constructed dataset adheres to a standardized instruction format, as depicted in Table 1 #1, comprising Text-SVG pairs for fine-tuning in text-to-SVG generation tasks. For text-guided SVG synthesis, visual prompts are indispensable. As illustrated in Table 1 #2, Text-Image-SVG triples facilitate instruction tuning for text-and-image to SVG generation.

During the SVG re-captioning phase, we obtained the corresponding text descriptions from the BLIP based on the rendering results, which were sufficient for text prompts, but too short for comments to understand SVG. Inspired by the recent success of GPT models in text annotation tasks [12], we utilized ChatGPT/GPT-4 for instruction-following data generation.

In total, we collected a dataset consisting of 250k annotated, high-quality, and standardized vector graphics, along with 580k unique SVG-Text-Image samples. The distribu-



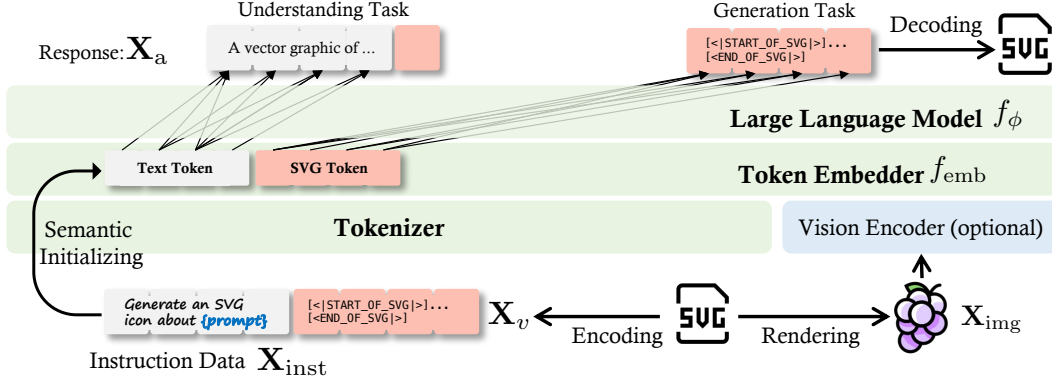


Figure 2. **An Overview of LLM4SVG.** Our LLM4SVG is capable of understanding and generating SVGs effectively. (1) During the training phase, we provide both the original SVG code  $\mathbf{X}_v$  and the corresponding instruction data  $\mathbf{X}_{inst}$  as input. For the understanding task, we use detailed descriptions  $\mathbf{X}_a$  generated by GPT-4 [2] as the training labels. For the generation task, the SVG code portion is masked and serves as the target that the model needs to predict. (2) During the inference phase, for the understanding task, given an SVG source code, the model generates a description that aligns with the semantics expressed by the SVG. For the generation task, the model generates an SVG based on the input text prompt. During both training and inference phases, the rendered image  $\mathbf{X}_{img}$  of the SVG can be used as conditional input to the model, guiding the content that the model understands or generates.

tion across sample types is as follows: 250k samples of type #1, which extend to 250k samples of type #2, 60k samples of type #3 and #4, and 20k samples of type #5.

## 4. Instruction Tuning Scheme

We then delve into the architecture of LLM4SVG, which takes as input an SVG and user instruction and outputs responses. We first introduce the definition of a semantic token, and then introduce the two-stage training strategy.

### 4.1. SVG Semantic Tokens

For an input SVG  $\mathbf{X}_v$ , we convert it from raw code into a structured representation. To accomplish this, we defined 55 SVG semantic tokens  $s_i \in \mathbb{R}^{55}$  (including 15 tag tokens, 30 attribute tokens, 10 path command tokens). These SVG tokens are used to replace all tags and attributes in the SVG source code, thus preventing the textual encoding of SVG tags and attributes as regular text. For example, the tag `<path>` will be tokenized as an SVG semantic token, rather than the literal “path” by the tokenizer. This ensures the uniqueness of SVG tags and attributes, and allows for their efficient integration into LLMs in a manner that is consistent with SVG definitions and optimizes token initialization. We adapt the embedding layer  $\mathbf{W}_{emb} \in \mathbb{R}^{|\mathcal{V}'|}$  to learn the embeddings of these new tokens, where  $|\mathcal{V}'| := |\mathcal{V}| + 55$  represents the sum of the size of the original vocabulary and the additional SVG tokens. Each new token is initialized based on the semantic average of its descriptive text, as defined by the equation:

$$\mathbf{E}(s_i) = \frac{1}{n} \sum_{j=1}^n \mathbf{W}_{emb}^\top \cdot w_{i,j} \quad (1)$$

where  $w_{i,j}$  represents the  $j$ -th description token of  $i$ -th  $s_i$ ,  $\mathbf{E}(\cdot)$  represents the token embedding layer and  $n = 55$ . This initialization provides a good starting point for each SVG token and builds a compact, distributed representation for all SVG tokens.

### 4.2. Architecture

The primary goal is to effectively leverage the capabilities of both the pre-trained LLMs and visual models. The network architecture is illustrated in Fig. 2. We chose GPT-2 [39], Phi-2 [24, 32] and Falcon [3] as the foundational LLMs for our framework, denoted as  $f_\phi$  and parameterized by  $\phi$ . These models were chosen because they possess the ability to understand both visual and textual data, and they demonstrate effective instruction-following properties in various language tasks among existing open source models. Theoretically, other LLMs with similar capabilities could also serve as the bases for our method.

### 4.3. Training

For each SVG  $\mathbf{X}_v$ , we sample multi-turn conversation data  $(\mathbf{X}_{un}^1, \mathbf{X}_{gen}^1, \dots, \mathbf{X}_{un}^T, \mathbf{X}_{gen}^T)$  from our SVG instruction dataset, where  $\mathbf{X}_{un}$  represents the understanding tasks and  $\mathbf{X}_{gen}$  refers to the generation tasks.  $T$  denotes the total number of turns in the conversation.

We apply instruction-tuning to the LLM using its original auto-regressive training objective for enhancing its performance on prediction tasks. Specifically, for a sequence of length  $L$ , we compute the probability of the target answers  $\mathbf{X}_a$  using the following equation:

$$p(\mathbf{X}_a | \mathbf{X}_v, \mathbf{X}_{inst}) = \prod_{i=1}^L p_\theta(\mathbf{x}_i | \mathbf{X}_v, \mathbf{X}_{inst}, \mathbf{X}_a, \hat{\mathbf{x}}_{i-1}) \quad (2)$$

Method / Metric	Type	Visual Metric				Latency
		FID↓	CLIPScore↑	Aesthetic↑	HPS↑	Gen. Time↓
CLIPDraw [11]	Optim-based	132.75	0.2486	3.9803	0.2347	5min20s
Evolution [54]	Optim-based	123.97	0.1932	4.0845	0.1955	49min42s
DiffSketcher[66]	Optim-based	77.35	0.2402	4.1562	0.2423	12min9s
LIVE+VectorFusion [23]	Optim-based	84.71	0.2298	4.5165	0.2334	32min19s
VectorFusion [23]	Optim-based	87.73	0.2720	4.9845	0.2450	11min27s
SVGDreamer [67]	Optim-based	72.68	0.3001	5.5432	0.2685	43min56s
SVG-VAE [29]	NN-based	79.25	0.1893	2.674	0.098	1min4s
DeepSVG [4]	NN-based	71.37	0.2118	3.0017	0.109	2min3s
Iconshop [63]	NN-based	85.45	0.2489	3.4682	0.1376	1min8s
StrokeNUWA [51]	NN-based	92.31	0.3001	5.5432	0.1659	20s
StarVector [43]†	LLM-based	112.89	0.3108	5.5157	0.1977	25s
LLM4SVG(GPT-2 small)	LLM-based	78.10	0.3129	5.7327	0.2076	12s
LLM4SVG(GPT-2 large)	LLM-based	66.09	0.3205	5.8729	0.2190	14s
LLM4SVG(GPT-2-XL)	LLM-based	64.11	0.3496	5.9836	0.2485	18s
LLM4SVG(Phi-2)	LLM-based	65.98	0.3373	5.9124	0.2289	20s
LLM4SVG(Falcon)	LLM-based	77.13	0.3018	4.9846	0.2012	25s
LLM4SVG(LLaVA)	LLM-based	66.72	0.3296	5.6846	0.2177	25s

(a) **Quantitative Comparison Between LLM4SVG and State-of-the-Art Text-to-SVG Methods.** †: Results from our reproduction.

Model	Input	FID↓	CLIPScore↑	Aesthetic↑	HPS↑	Avg.Tok
Llama-3.1 70B [10]	Text	138.44	0.2735	4.3048	0.1665	707.67
Gemini-1.5 Pro [7]	Text&Img	145.76	0.2622	4.2708	0.1511	547.50
Claude-3.5 [35]	Text	82.89	0.3083	5.2370	0.1912	736.38
Yi-1.5 34B [70]	Text	140.83	0.2824	4.5118	0.1676	633.42
Grok-2 [65]	Text	116.99	0.2840	4.8086	0.1663	581.88
Qwen2.5 70B [52]	Text	131.46	0.2803	4.5024	0.1691	705.00
GPT-3.5 [34]	Text&Img	129.40	0.2949	4.3070	0.1717	530.59
GPT-4o [2]	Text&Img	127.78	0.2949	5.0262	0.1788	654.12
GPT-4o1-preview [2]	Text&Img	135.33	0.2968	4.7754	0.1840	755.71
LLM4SVG(GPT-2 XL)	Text	64.11	0.3496	5.9836	0.2485	2297.75
LLM4SVG(Falcon)	Text	77.13	0.3018	4.9846	0.2012	1829.49
LLM4SVG(LLaVA)	Text&Img	66.72	0.3296	5.6846	0.2177	2009.41

(b) **Quantitative Comparison Between LLM4SVG and State-of-the-Art LLMs.**

Table 2. **Quantitative Comparison of LLM4SVG.** (a) is used to indicate comparisons against SVG generation methods. (b) is employed to compare performance with LLM-based methods.

where  $\theta$  represents the trainable parameters of the model,  $\mathbf{X}_{\text{inst}}$  and  $\mathbf{X}_a$  are the tokens corresponding to the instructions and answers for all preceding turns before the current prediction token  $x_i$ , respectively. The term  $\hat{x}_{i-1} = x_{i-1}, \dots, x_1$  denotes the sequence of tokens that have been predicted in previous steps.

**Stage 1: Pre-training for Feature Alignment.** These pairs are converted to instruction-following data using the naive expansion method describe in Sec. 3. Each sample can be treated as a single-turn conversation. To construct the input  $\mathbf{X}_{\text{inst}}$ , instruction data is randomly sampled. In training, we keep the weights of both the visual encoder and the LLM frozen, and focus on maximizing the likelihood of Eq. 2 with trainable parameters  $\theta = \mathbf{W}_{\text{emb}}$  (the word embedding) only.

**Stage 2: Fine-tuning End-to-End.** We employ the entire instruction dataset for supervised fine-tuning of all parameters, including those of the LLM, *i.e.*, the trainable parameters are  $\theta = \{\mathbf{W}_{\text{emb}}, \phi\}$  in Eq. 2. We consider two specific use case scenarios:

- *Efficient parameters fine-tuning.* Methods like LoRA [9, 19] only fine-tune a small number of additional model parameters, significantly decreasing computational and storage costs while delivering performance comparable to that of a fully fine-tuned model. This approach facilitates the training and storage of LLMs on consumer hardware.
- *Full fine-tuning.* Fine-tuning all parameters requires higher computational resources, especially in large language models.

## 5. Experiments

**Overview.** This section outlines the core aspects of our model implementation, followed by a description of the dataset collection and preprocessing pipeline, which involves 250,000 high-quality SVG files. We then empiri-

cally evaluate the effectiveness of our model, LLM4SVG, in generating high-quality SVGs. This evaluation benchmarks our model against current state-of-the-art methods both qualitatively and quantitatively, as detailed in Sec. 5.1 and 5.2. This evaluation is augmented with a comprehensive architectural analysis, including ablation studies detailed in Sec. 5.3, to identify the specific contributions of individual model components to the overall performance.

**Implementation Details.** In the initial stage of training, we exclusively focus on the word embeddings  $\mathbf{W}_{\text{emb}}$ . As mentioned in Sec. 4.1, we added 55 SVG semantic tokens and initialized the word embedding using the semantic average of the description text.

In the second stage, we employ an end-to-end fine-tuning strategy to comprehensively optimize model performance. For the LoRA [19] and QLoRA [9] approaches, we configure the LoRA rank  $r = 32$  and scaling factor  $\alpha = 32$ .

During both training stages, we apply the AdamW optimizer with hyper-parameters  $\beta_1 = 0.9, \beta_2 = 0.999, \epsilon = 1 \times 10^{-8}$ , and a learning rate of  $lr = 2 \times 10^{-5}$ . We also address the potential complexity of certain SVG structures by setting a maximum token length of 2048. If an SVG’s token sequence exceeds this length, it is directly truncated to the maximum length. This approach prevents excessive sequence lengths that could hinder training efficiency and ensures the model remains within manageable computational limits. Training was performed using 8 NVIDIA A800 GPUs.

**Datasets.** Our dataset comprise 250,000 emoji and icon SVGs, sourced from TwEmoji [56], NotoEmoji [14], FluentUIEmoji [31], as well as SVGRepo [50] and Reshot [42] websites. Specifically, the TwEmoji, NotoEmoji, and FluentUIEmoji subsets each contain approximately 3,000–4,000 SVGs. The Reshot website contributes 30,000 SVGs, while SVGRepo provides the remaining

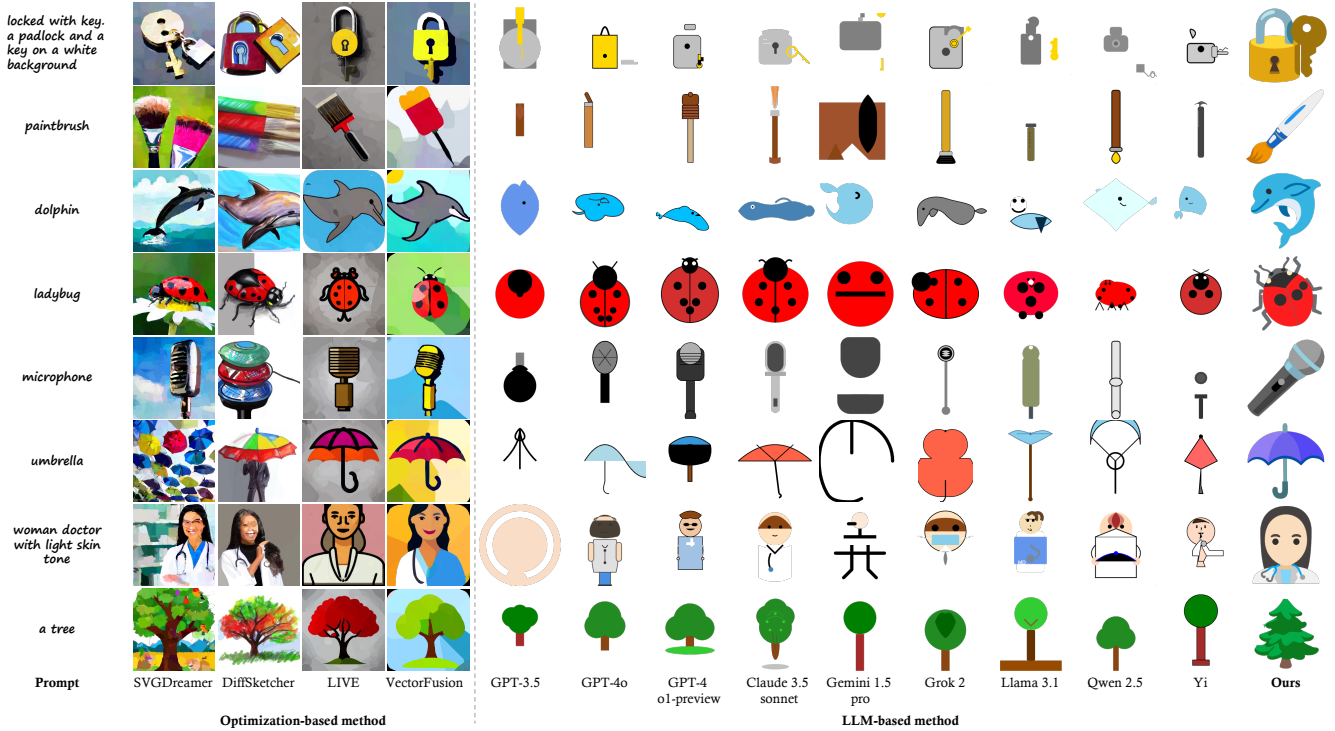


Figure 3. **Qualitative Comparison Between LLM4SVG and State-of-the-Art SVG Generation Methods**, including optimization-based and LLM-based methods.

210,000. As mentioned earlier, after collecting the SVG files, we preprocess them to enhance training efficiency and ensure consistency. **Evaluation Metrics.** To facilitate a comprehensive assessment of our proposed method compared to baseline approaches, we classify all methods into three categories: Optimization-based methods, Neural Network-based methods, and LLM-based methods. We then evaluate these methods across two key dimensions: visual quality and computational cost. For visual quality, we measure (1) visual quality using FID (Fréchet Inception Distance)[17]; (2) text prompt alignment through the CLIP score [40]; and (3) aesthetic appeal using the Aesthetic score [46] and HPS (Human Preference Scores) [64]. (4) for computational cost, we test and compare the time cost of generating 10 SVGs by each method. (5) Avg.Tok represents the length of SVG code after removing comments and whitespace.

### 5.1. Quantitative Evaluation

Table 2a presents a comparison of our approach with the most prominent text-to-SVG baseline methods across the previously defined dimensions. Our LLM4SVG model achieves the highest performance among LLM-based SVG generation methods. While it may not surpass optimization-based methods in terms of visual quality, it remains competitive, closely matching the performance of other methods across several evaluation metrics. Furthermore, our ap-

proach only requires model inference, eliminating the need for a time-consuming optimization process, which results in a significantly shorter SVG generation time compared to optimization-based methods.

As shown in Table 2b, our LLM4SVG outperforms all other LLMs across every aspect. Moreover, due to the limited support for continuous numerical data in most LLMs, SVGs generated by these models often exhibit imprecise coordinates and color representations, typically relying on integers rather than decimals and using basic color names like black or blue, instead of more precise hexadecimal codes. Our approach addresses these shortcomings by incorporating decimal coordinates and hexadecimal color codes for SVG paths, thereby expanding the model’s ability to represent a wider and more accurate range of colors (as illustrated in Fig. S1). Further comparisons with LLM-based methods are provided in Sec. A of Supplementary.

### 5.2. Qualitative Evaluation

Figure 3 illustrates the visual quality of SVG generation methods, comparing both optimization-based and LLM-based approaches. It is evident that our method outperforms other LLM-based methods in terms of the completeness of the SVG generation, the selection and placement of primitives, and the semantic richness conveyed by the vector graphics. Optimization-based methods [11, 23, 54, 66, 67] use samples from the Latent Diffusion Model as supervision

Metric/Method	GPT4-o [2]	Claude-3.5 [35]	LLM4SVG	Human SVG
Prompt Alignment	0.49	0.56	0.89	0.94
Visual Quality	0.61	0.74	0.92	0.95
Pick Score	0.57	0.69	0.88	0.92

Table 3. **Results of Human Evaluation.** *Human SVG* refers to the SVGs designed by human designers in our collected dataset.

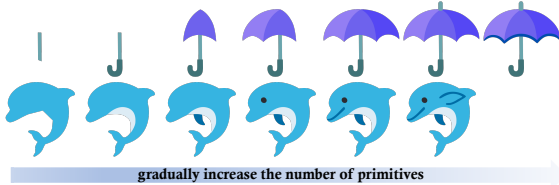


Figure 4. **Our LLM4SVG Model Generates SVGs with Primitive Ordering that Aligns with Human Design Principles.** The upper example demonstrates a gradual design process, progressing from individual components to the complete design. In contrast, the lower example begins with the overall design before detailing each individual component.

during the SVG generation process. Consequently, these methods normally employ a large number of overlapping and interwoven primitives to closely approximate the realistic samples. This often lead to excessive stroke redundancy, and the individual shapes of the primitives may appear irregular when viewed in isolation, making them less practical for use in real-life applications. In Fig. S7, we show more SVGs generated by our LLM4SVG.

**Human Evaluation.** To evaluate the visual effects of our generated SVGs compared to other LLMs, we conducted a user study. As Claude 3.5 and GPT-4 are currently recognized as two of the best LLMs, we compared SVGs generated by our LLM4SVG with those produced by these models. In this study, we shuffled the SVGs generated by the different models together with the selected examples from our dataset. Participants were only provided with the text descriptions and the shuffled SVGs. They were then asked to evaluate the SVGs based on prompt alignment, visual quality, and their willingness to use the SVGs in real-world scenarios. The results are presented in Table 3, where our generated SVGs significantly outperformed other LLM-based methods, and the visual quality of our SVGs is closely comparable to that of SVGs created by humans. Further details of human evaluation are provided in Sec. C of Supplementary.

### 5.3. Ablation Study

**Analysis of the LLM4SVG Architecture.** The performance of LLM4SVG is significantly influenced by the underlying base model, especially concerning how the LLM tokenizer manages continuous numeric tokens. For example, in the Qwen models [52, 59], during the tokenization process, all numbers and decimal points are converted into

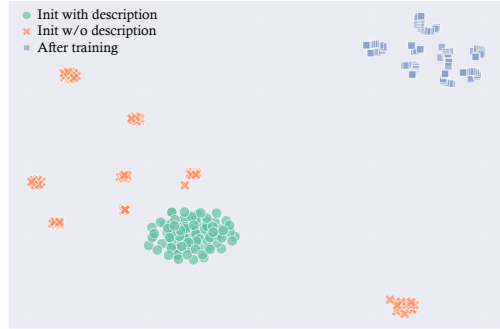


Figure 5. **t-SNE Visualization of Token Embeddings.** The green dots represent the SVG token embeddings initialized with descriptions, while the yellow crosses indicate those initialized without descriptions. The blue squares represent SVG token embeddings after training.

a single token. As a result, Qwen is unable to properly handle continuous numerical data, leading to poor performance in tasks such as coordinate and hexadecimal color prediction, making it difficult to generate complete and coherent SVGs. LLMs like GPT-2 [39], which enumerate all numbers within 1000 as individual tokens in the tokenizer, exhibit a stronger understanding of numerical data. This capability allows such models to generate more complete and coherent SVGs, leading to a more visually appealing and harmonious output.

**Analysis of SVG Semantic Tokens.** During the model training process, we expanded the tokenizer by incorporating 55 SVG-specific semantic tokens. This modification enables SVG tags and attributes to be identified with distinct tokens, thereby differentiating them from general text. For instance, prior to this addition, the word `path` could ambiguously refer to an SVG tag or merely a physical path. However, with the introduction of a dedicated `path` token, the model is now equipped to clearly differentiate between the SVG path tag and a literal path. This distinction aids the model in more effectively and accurately learning the SVG generation template, enhancing its ability to produce precise and contextually appropriate SVGs.

**Analysis of Word Embedding Initialization Method.** As illustrated in Fig. 5, we used T-SNE [57] to map the newly added tokens into a two-dimensional visualization for better demonstration. In this visualization, the green dots represent tokens that were initialized using the text description of each token. Specifically, we averaged the values obtained from tokenizing these descriptions to initialize the tokens, a process detailed in Sec. 4.1. This strategy groups the token embeddings into a relatively compact region within the feature space, which helps reduce the difficulty of model training. The yellow crosses, on the other hand, indicate tokens that were initialized without using the text description. These tokens exhibits a more scattered distribu-



tion across the feature space, making it challenging for the model to learn the accurate meaning of these tokens. The blue squares represent the positions of the tokens within the feature space post-training. It is evident that after the training phase, the token embeddings not only maintain local continuity, evidenced by smooth transitions within clusters, but also exhibit a reasonable of discreteness, where different functional SVG elements form distinct clusters. Additionally, these tokens remain closely within the overall feature space. This visualization demonstrates the rationale behind our token addition method and the effectiveness of our training approach.

## 6. Conclusion & Discussion

In this work, we proposed a method that harnesses the capabilities of Large Language Models (LLMs) for both understanding and generating SVGs, enabling LLMs to directly interpret SVG source code and generate high-quality SVGs. These generated SVGs exhibit a certain level of complexity, and align with human design principles. Our method introduces a structured SVG encoding approach that addresses the challenge of LLMs treating SVG source code as ordinary text. Traditionally, this treatment often results in inefficient use of tokens for learning SVG structures and numerical encoding, thereby complicating model training. Additionally, we have collected a dataset consisting of 250,000 high-quality SVGs designed by human designers and 580,000 SVG-text instruction pairs. This dataset is expected to significantly expedite the future research related to vector graphics.

**Future Work.** Our LLM4SVG can leverage different LLMs as its base model. In the future, more advanced and complex models could serve as the base, and combined with multimodal large language model to integrate image information. This extension may help reduce the difficulty of model understanding and generation, enabling more accurate and efficient SVG generation.

## References

- [1] Marah Abdin, Jyoti Aneja, Hany Awadalla, Ahmed Awadallah, Ammar Ahmad Awan, Nguyen Bach, Amit Bahree, Arash Bakhtiari, Jianmin Bao, Harkirat Behl, et al. Phi-3 technical report: A highly capable language model locally on your phone. *arXiv preprint arXiv:2404.14219*, 2024. 3
- [2] Josh Achiam, Steven Adler, Sandhini Agarwal, Lama Ahmad, Ilge Akkaya, Florencia Leoni Aleman, Diogo Almeida, Janko Altenschmidt, Sam Altman, Shyamal Anadkat, et al. Gpt-4 technical report. *arXiv preprint arXiv:2303.08774*, 2023. 2, 3, 4, 5, 6, 8, 13, 14, 15
- [3] Ebtesam Almazrouei, Hamza Alobeidli, Abdulaziz Alshamsi, Alessandro Cappelli, Ruxandra Cojocaru, M erouane Debbah,  tienne Goffinet, Daniel Hesslow, Julien Launay, Quentin Malartic, et al. The falcon series of open language models. *arXiv preprint arXiv:2311.16867*, 2023. 3, 5
- [4] Alexandre Carlier, Martin Danelljan, Alexandre Alahi, and Radu Timofte. Deepsvg: A hierarchical generative network for vector graphics animation. *Advances in Neural Information Processing Systems (NeurIPS)*, 33:16351–16361, 2020. 2, 3, 6
- [5] Mark Chen, Jerry Tworek, Heewoo Jun, Qiming Yuan, Henrique Ponde De Oliveira Pinto, Jared Kaplan, Harri Edwards, Yuri Burda, Nicholas Joseph, Greg Brockman, et al. Evaluating large language models trained on code. *arXiv preprint arXiv:2107.03374*, 2021. 2
- [6] Louis Clou tre and Marc Demers. Figr: Few-shot image generation with reptile. *arXiv preprint arXiv:1901.02199*, 2019. 3
- [7] DeepMind. Gemini pro. <https://deepmind.google/technologies/gemini/pro/>, 2024. 3, 6, 13
- [8] Soham Deshmukh, Benjamin Elizalde, Rita Singh, and Huaming Wang. Pengi: An audio language model for audio tasks. In *Thirty-seventh Conference on Neural Information Processing Systems (NeurIPS)*, 2023. 3
- [9] Tim Dettmers, Artidoro Pagnoni, Ari Holtzman, and Luke Zettlemoyer. Qlora: Efficient finetuning of quantized llms. *Advances in Neural Information Processing Systems*, 36, 2024. 6
- [10] Abhimanyu Dubey, Abhinav Jauhri, Abhinav Pandey, Abhishek Kadian, Ahmad Al-Dahle, Aiesha Letman, Akhil Mathur, Alan Schelten, Amy Yang, Angela Fan, et al. The llama 3 herd of models. *arXiv preprint arXiv:2407.21783*, 2024. 6, 13
- [11] Kevin Frans, Lisa Soros, and Olaf Witkowski. CLIPDraw: Exploring text-to-drawing synthesis through language-image encoders. In *Advances in Neural Information Processing Systems (NeurIPS)*, 2022. 2, 3, 6, 7
- [12] Fabrizio Gilardi, Meysam Alizadeh, and Ma l Kubli. Chatgpt outperforms crowd workers for text-annotation tasks. *Proceedings of the National Academy of Sciences*, 120(30), 2023. 4
- [13] Tao Gong, Chengqi Lyu, Shilong Zhang, Yudong Wang, Miao Zheng, Qianmengke Zhao, Kuikun Liu, Wenwei Zhang, Ping Luo, and Kai Chen. Multimodal-gpt: A vision and language model for dialogue with humans. *ArXiv*, abs/2305.04790, 2023. 3
- [14] Google. Noto emoji fonts. <https://github.com/googlefonts/noto-emoji>, 2014. 6
- [15] Tanmay Gupta and Aniruddha Kembhavi. Visual programming: Compositional visual reasoning without training. In *Proceedings of the IEEE/CVF Conference on Computer Vision and Pattern Recognition (CVPR)*, pages 14953–14962, 2023. 3
- [16] David Ha and Douglas Eck. A neural representation of sketch drawings. In *International Conference on Learning Representations (ICLR)*, 2018. 2
- [17] Martin Heusel, Hubert Ramsauer, Thomas Unterthiner, Bernhard Nessler, and Sepp Hochreiter. Gans trained by a

- two time-scale update rule converge to a local nash equilibrium. *Advances in neural information processing systems (NeurIPS)*, 30, 2017. 7
- [18] Yining Hong, Haoyu Zhen, Peihao Chen, Shuhong Zheng, Yilun Du, Zhenfang Chen, and Chuang Gan. 3d-LLM: Injecting the 3d world into large language models. In *Thirty-seventh Conference on Neural Information Processing Systems*, 2023. 3
- [19] Edward J Hu, Yelong Shen, Phillip Wallis, Zeyuan Allen-Zhu, Yuanzhi Li, Shean Wang, Lu Wang, and Weizhu Chen. Lora: Low-rank adaptation of large language models. *arXiv preprint arXiv:2106.09685*, 2021. 6
- [20] Teng Hu, Ran Yi, Baihong Qian, Jiangning Zhang, Paul L Rosin, and Yu-Kun Lai. Supersvg: Superpixel-based scalable vector graphics synthesis. In *Proceedings of the IEEE/CVF Conference on Computer Vision and Pattern Recognition (CVPR)*, pages 24892–24901, 2024. 2, 3
- [21] Rongjie Huang, Mingze Li, Dongchao Yang, Jiatong Shi, Xuankai Chang, Zhenhui Ye, Yuning Wu, Zhiqing Hong, Jiawei Huang, Jinglin Liu, Yi Ren, Zhou Zhao, and Shinji Watanabe. Audiogpt: Understanding and generating speech, music, sound, and talking head, 2023. 3
- [22] Shaohan Huang, Li Dong, Wenhui Wang, Yaru Hao, Saksham Singhal, Shuming Ma, Tengchao Lv, Lei Cui, Owais Khan Mohammed, Barun Patra, Qiang Liu, Kriti Aggarwal, Zewen Chi, Johan Bjorck, Vishrav Chaudhary, Subhojit Som, Xia Song, and Furu Wei. Language is not all you need: Aligning perception with language models. In *Thirty-seventh Conference on Neural Information Processing Systems (NeurIPS)*, 2023. 3
- [23] Ajay Jain, Amber Xie, and Pieter Abbeel. Vectorfusion: Text-to-svg by abstracting pixel-based diffusion models. In *Proceedings of the IEEE/CVF Conference on Computer Vision and Pattern Recognition (CVPR)*, 2023. 2, 3, 6, 7
- [24] Mojan Javaheripi, Sébastien Bubeck, Marah Abdin, Jyoti Aneja, Sébastien Bubeck, Caio César Teodoro Mendes, Weizhu Chen, Allie Del Giorno, Ronen Eldan, Sivakanth Gopi, et al. Phi-2: The surprising power of small language models. *Microsoft Research Blog*, 1:3, 2023. 3, 5
- [25] Biao Jiang, Xin Chen, Wen Liu, Jingyi Yu, Gang YU, and Tao Chen. MotionGPT: Human motion as a foreign language. In *Thirty-seventh Conference on Neural Information Processing Systems (NeurIPS)*, 2023. 3
- [26] Junnan Li, Dongxu Li, Caiming Xiong, and Steven C. H. Hoi. Blip: Bootstrapping language-image pre-training for unified vision-language understanding and generation. In *International Conference on Machine Learning (ICML)*, 2022. 4, 15
- [27] Tzu-Mao Li, Michal Lukáč, Gharbi Michaël, and Jonathan Ragan-Kelley. Differentiable vector graphics rasterization for editing and learning. *ACM Transactions on Graphics (TOG)*, 39(6):193:1–193:15, 2020. 2, 3
- [28] Haotian Liu, Chunyuan Li, Qingyang Wu, and Yong Jae Lee. Visual instruction tuning. In *Advances in Neural Information Processing Systems (NeurIPS)*, pages 34892–34916, 2023. 2, 3
- [29] Raphael Gontijo Lopes, David Ha, Douglas Eck, and Jonathon Shlens. A learned representation for scalable vector graphics. In *Proceedings of the IEEE/CVF International Conference on Computer Vision (ICCV)*, 2019. 2, 3, 6
- [30] Xu Ma, Yuqian Zhou, Xingqian Xu, Bin Sun, Valerii Filev, Nikita Orlov, Yun Fu, and Humphrey Shi. Towards layer-wise image vectorization. In *Proceedings of the IEEE/CVF Conference on Computer Vision and Pattern Recognition (CVPR)*, pages 16314–16323, 2022. 3
- [31] Microsoft. Fluent emoji. <https://github.com/microsoft/fluentui-emoji>, 2021. 6
- [32] microsoft phi2 team. Phi-2: The surprising power of small language models. [https://nips.cc/media/neurips-2023/Slides/83968\\_5GxuY2z.pdf](https://nips.cc/media/neurips-2023/Slides/83968_5GxuY2z.pdf), 2023. 3, 5
- [33] Piotr Mirowski, Dylan Banarse, Mateusz Malinowski, Simon Osindero, and Chrisantha Fernando. Clip-clop: Clip-guided collage and photomontage. *arXiv preprint arXiv:2205.03146*, 2022. 2, 3
- [34] OpenAI. Introducing chatgpt. <https://openai.com/index/chatgpt/>, 2023. 2, 3, 6, 13
- [35] OpenAI. Claude 3.5 sonnet. <https://www.anthropic.com/news/claude-3-5-sonnet>, 2024. 3, 6, 8, 13, 14
- [36] Long Ouyang, Jeffrey Wu, Xu Jiang, Diogo Almeida, Carroll Wainwright, Pamela Mishkin, Chong Zhang, Sandhini Agarwal, Katarina Slama, Alex Ray, et al. Training language models to follow instructions with human feedback. *Advances in neural information processing systems*, 35:27730–27744, 2022. 3
- [37] Shishir G. Patil, Tianjun Zhang, Xin Wang, and Joseph E. Gonzalez. Gorilla: Large language model connected with massive apis. *arXiv preprint arXiv:2305.15334*, 2023. 3
- [38] Ben Poole, Ajay Jain, Jonathan T. Barron, and Ben Mildenhall. Dreamfusion: Text-to-3d using 2d diffusion. In *The Eleventh International Conference on Learning Representations (ICLR)*, 2023. 2
- [39] Alec Radford, Jeff Wu, Rewon Child, David Luan, Dario Amodei, and Ilya Sutskever. Language models are unsupervised multitask learners. 2019. 2, 5, 8
- [40] Alec Radford, Jong Wook Kim, Chris Hallacy, Aditya Ramesh, Gabriel Goh, Sandhini Agarwal, Girish Sastry, Amanda Askell, Pamela Mishkin, Jack Clark, et al. Learning transferable visual models from natural language supervision. In *International Conference on Machine Learning (ICML)*, pages 8748–8763. PMLR, 2021. 3, 7
- [41] Pradyumna Reddy, Michael Gharbi, Michal Lukac, and Niloy J Mitra. Im2vec: Synthesizing vector graphics without vector supervision. In *Proceedings of the IEEE/CVF Conference on Computer Vision and Pattern Recognition (CVPR)*, pages 7342–7351, 2021. 2
- [42] ReShot. Reshot: Free icons & illustrations. <https://www.reshot.com/>, 2016. 6
- [43] Juan A. Rodriguez, Shubham Agarwal, Issam H. Laradji, Pau Rodriguez, David Vazquez, Christopher Pal, and Marco Pedersoli. Starvector: Generating scalable vector graphics code from images, 2023. 2, 3, 6
- [44] Robin Rombach, Andreas Blattmann, Dominik Lorenz, Patrick Esser, and Björn Ommer. High-resolution image

- synthesis with latent diffusion models. In *Proceedings of the IEEE/CVF Conference on Computer Vision and Pattern Recognition (CVPR)*, pages 10684–10695, 2022. 2
- [45] Patsorn Sangkloy, Nathan Burnell, Cusuh Ham, and James Hays. The sketchy database: learning to retrieve badly drawn bunnies. *ACM Trans. Graph.*, 35(4), 2016. 3
- [46] Christoph Schuhmann. Improved aesthetic predictor. <https://github.com/christophschuhmann/improved-aesthetic-predictor>, 2022. 7
- [47] I-Chao Shen and Bing-Yu Chen. Clipgen: A deep generative model for clipart vectorization and synthesis. *IEEE Transactions on Visualization and Computer Graphics*, 28(12):4211–4224, 2022. 3
- [48] Yiren Song, Xuning Shao, Kang Chen, Weidong Zhang, Zhongliang Jing, and Minzhe Li. Clipvg: Text-guided image manipulation using differentiable vector graphics. In *Proceedings of the Conference on Artificial Intelligence (AAAI)*, 2023.
- [49] Hao Su, Xuefeng Liu, Jianwei Niu, Jiahe Cui, Ji Wan, Xinghao Wu, and Nana Wang. Marvel: Raster gray-level manga vectorization via primitive-wise deep reinforcement learning. *IEEE Transactions on Circuits and Systems for Video Technology (T-CSVT)*, 2023. 3
- [50] SVGRepo. Open-licensed svg vector and icons. <https://www.svgrepo.com/>, 2016. 6
- [51] Zecheng Tang, Chenfei Wu, Zekai Zhang, Mingheng Ni, Shengming Yin, Yu Liu, Zhengyuan Yang, Lijuan Wang, Zicheng Liu, Juntao Li, et al. Strokenuwa: Tokenizing strokes for vector graphic synthesis. *arXiv preprint arXiv:2401.17093*, 2024. 2, 6
- [52] Qwen Team. Qwen2.5: A party of foundation models, 2024. 3, 6, 8, 13
- [53] Vikas Thamizharasan, Difan Liu, Matthew Fisher, Nanxuan Zhao, Evangelos Kalogerakis, and Michal Lukac. Nivel: Neural implicit vector layers for text-to-vector generation. In *Proceedings of the IEEE/CVF Conference on Computer Vision and Pattern Recognition (CVPR)*, pages 4589–4597, 2024. 2, 3
- [54] Yingtao Tian and David Ha. Modern evolution strategies for creativity: Fitting concrete images and abstract concepts. In *Artificial Intelligence in Music, Sound, Art and Design*, pages 275–291. Springer, 2022. 3, 6, 7
- [55] Hugo Touvron, Thibaut Lavril, Gautier Izacard, Xavier Martinet, Marie-Anne Lachaux, Timothée Lacroix, Baptiste Rozière, Naman Goyal, Eric Hambro, Faisal Azhar, Aurelien Rodriguez, Armand Joulin, Edouard Grave, and Guillaume Lample. Llama: Open and efficient foundation language models. *ArXiv*, abs/2302.13971, 2023. 2, 3, 13
- [56] Twitter. Twitter color emoji svginot font. <https://github.com/13rac1/twemoji-color-font>, 2016. 6
- [57] Laurens Van der Maaten and Geoffrey Hinton. Visualizing data using t-sne. *Journal of machine learning research*, 9(11), 2008. 8
- [58] Yael Vinker, Ehsan Pajouheshgar, Jessica Y Bo, Roman Christian Bachmann, Amit Haim Bermano, Daniel Cohen-Or, Amir Zamir, and Ariel Shamir. Clipasso: Semantically-aware object sketching. *ACM Transactions on Graphics (TOG)*, 41(4):1–11, 2022. 2, 3
- [59] Peng Wang, Shuai Bai, Sinan Tan, Shijie Wang, Zhihao Fan, Jinze Bai, Keqin Chen, Xuejing Liu, Jialin Wang, Wenbin Ge, et al. Qwen2-vl: Enhancing vision-language model’s perception of the world at any resolution. *arXiv preprint arXiv:2409.12191*, 2024. 3, 8, 13
- [60] Wenhai Wang, Zhe Chen, Xiaokang Chen, Jiannan Wu, Xizhou Zhu, Gang Zeng, Ping Luo, Tong Lu, Jie Zhou, Yu Qiao, and Jifeng Dai. VisionLLM: Large language model is also an open-ended decoder for vision-centric tasks. In *Thirty-seventh Conference on Neural Information Processing Systems (NeurIPS)*, 2023. 3
- [61] Yizhi Wang and Zhouhui Lian. Deepvecfont: Synthesizing high-quality vector fonts via dual-modality learning. *ACM Transactions on Graphics (TOG)*, 40(6), 2021. 2, 3
- [62] Yizhong Wang, Yeganeh Kordi, Swaroop Mishra, Alisa Liu, Noah A Smith, Daniel Khashabi, and Hannaneh Hajishirzi. Self-instruct: Aligning language models with self-generated instructions. *arXiv preprint arXiv:2212.10560*, 2022. 3
- [63] Ronghuan Wu, Wanchao Su, Kede Ma, and Jing Liao. Iconshop: Text-based vector icon synthesis with autoregressive transformers. *arXiv preprint arXiv:2304.14400*, 2023. 2, 3, 6
- [64] Xiaoshi Wu, Keqiang Sun, Feng Zhu, Rui Zhao, and Hongsheng Li. Human preference score: Better aligning text-to-image models with human preference. In *Proceedings of the IEEE/CVF International Conference on Computer Vision (ICCV)*, pages 2096–2105, 2023. 7
- [65] xAI team. Grok-2 beta release. <https://x.ai/blog/grok-2>, 2024. 3, 6, 13
- [66] Ximing Xing, Chuang Wang, Haitao Zhou, Jing Zhang, Qian Yu, and Dong Xu. Diffsketcher: Text guided vector sketch synthesis through latent diffusion models. In *Advances in Neural Information Processing Systems (NeurIPS)*, 2023. 2, 3, 6, 7
- [67] Ximing Xing, Haitao Zhou, Chuang Wang, Jing Zhang, Dong Xu, and Qian Yu. Svgdreamer: Text guided svg generation with diffusion model. In *Proceedings of the IEEE/CVF Conference on Computer Vision and Pattern Recognition (CVPR)*, pages 4546–4555, 2024. 2, 3, 6, 7
- [68] Runsen Xu, Xiaolong Wang, Tai Wang, Yilun Chen, Jiangmiao Pang, and Dahua Lin. Pointllm: Empowering large language models to understand point clouds. In *ECCV*, 2024. 3
- [69] Zhongzheng Xu and Emily Wall. Exploring the capability of llms in performing low-level visual analytic tasks on svg data visualizations. *arXiv preprint arXiv:2404.19097*, 2024. 3
- [70] Alex Young, Bei Chen, Chao Li, Chengen Huang, Ge Zhang, Guanwei Zhang, Heng Li, Jiangcheng Zhu, Jianqun Chen, Jing Chang, et al. Yi: Open foundation models by 01. ai. *arXiv preprint arXiv:2403.04652*, 2024. 3, 6, 13
- [71] Qian Yu, Feng Liu, Yi-Zhe Song, Tao Xiang, Timothy M Hospedales, and Chen Change Loy. Sketch me that shoe. In *Computer Vision and Pattern Recognition (CVPR)*, pages 799–807. IEEE, 2016. 3

- [72] Hang Zhang, Xin Li, and Lidong Bing. Video-LLaMA: An instruction-tuned audio-visual language model for video understanding. In *Proceedings of the 2023 Conference on Empirical Methods in Natural Language Processing: System Demonstrations*, pages 543–553, Singapore, 2023. [3](#)
- [73] Peiying Zhang, Nanxuan Zhao, and Jing Liao. Text-to-vector generation with neural path representation. *arXiv preprint arXiv:2405.10317*, 2024. [2](#), [3](#)
- [74] Deyao Zhu, Jun Chen, Xiaoqian Shen, Xiang Li, and Mohamed Elhoseiny. MiniGPT-4: Enhancing vision-language understanding with advanced large language models. In *The Twelfth International Conference on Learning Representations (ICLR)*, 2024. [3](#)



# Empowering LLMs to Understand and Generate Complex Vector Graphics

## Supplementary Material

### Overview

In this supplementary material, we provide additional details and discussions related to our work on **LLM4SVG**. Specifically, it covers the following aspects:

- In Section A, we demonstrate the advantages of our approach over existing LLM-based methods for SVG generation, particularly in terms of visual appeal and the ability to handle numerical coordinates.
- In Section B, we show examples from our newly collected dataset and introduce a lossless preprocessing pipeline.
- In Section C, we provide more details about the user study, including the number of participants, their backgrounds, and how the metrics were obtained.
- In Section D, we present additional qualitative results of our LLM4SVG, showcasing its ability to generate SVGs with high editability and superior visual quality.

### A. Comparison with LLM-based Methods

Apart from Figure 3 in the manuscript, we present additional qualitative comparisons of our method with existing LLM-based methods in this section, including ChatGPT-3.5 [34], GPT-4o [2], GPT-o1-preview [2], Claude 3.5-sonnet [35], Gemini 1.5-pro [7], Grok 2 [65], Llama 3.1 [10, 55], Qwen 2.5 [52, 59], and Yi [70].

As illustrated in Fig.S3, it is evident that our proposed LLM4SVG outperforms other methods in terms of overall visual effect and detail expression. Specifically, most LLMs struggle to generate complete SVG images, for example, *butterfly*, or produce outputs that accurately align with the provided textual descriptions, such as *two-hump camel* illustrated in the last third example. Some recent LLMs perform relatively better, such as GPT-4o[2], GPT-o1-preview [2], and Claude 3.5-sonnet [35]. However, their results are still less satisfactory as the shapes are overly simplistic (e.g., *flute*) and the colors lack harmony (e.g., *a bed*). In contrast, the results of our LLM4SVG are more complete, with shapes that are more diverse, colors that are more harmonious, and semantics that are more closely aligned with the prompts.

Additionally, we compare the SVG source codes generated by our method and two of the most recent LLMs, GPT-o1-preview [2] and Claude 3.5-sonnet [35], to demonstrate the superiority of our method. As shown in Fig.S4, given the prompt “umbrella”, both GPT-o1-preview and Claude 3.5-sonnet can only predict integer coordinates, whereas our LLM4SVG is capable of generating precise decimal coordinates accurate to two decimal places. In the context of SVG representation, retaining only integer values can lead to in-

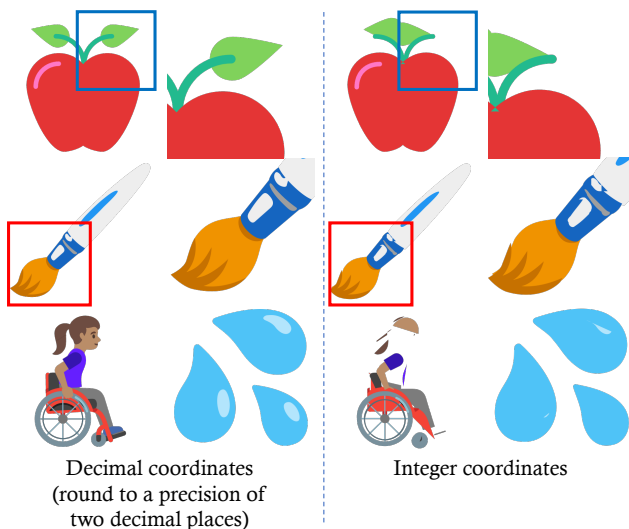


Figure S1. **Visual Comparison between Decimal Coordinates and Integer Coordinates in SVGs.** Only integer coordinates will lead to shape distortions and incompleteness.

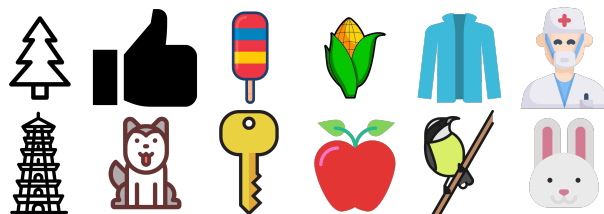


Figure S2. **Samples from Our Collected SVG Dataset.** Our collected datasets are extensive and highly diverse.

complete or distorted SVG shapes, as illustrated in Fig.S4. We present additional examples in Fig. S1 to further demonstrate the visual differences between integer and decimal coordinates.

### B. Dataset and Preprocessing Pipeline

In Fig. S2, we present examples from our extensive and diverse SVG dataset. This dataset includes primitives with varying levels of complexity, ranging from minimal to highly detailed, and utilizes a rich and harmonious color palette. Furthermore, it encompasses a wide range of subjects, including people, animals, objects, and symbols.

As discussed in Sec. 3 of our manuscript, approximately half of the data in an SVG file is redundant for visual rendering. Consequently, we introduce a lossless SVG preprocessing pipeline to streamline the dataset and enhance training

a bed										
boar. a cartoon boar head with a big nose.										
computer and keyboard										
butterfly										
two-hump camel. camel. cartoon vector illustration										
Santa Claus medium skin tone										
flute										
Prompt	GPT-3.5	GPT-4o	GPT-4 o1-preview	Claude 3.5 sonnet	Gemini 1.5 pro	Grok 2	Llama 3.1	Qwen 2.5	Yi	Ours

Figure S3. Qualitative Comparison of LLM4SVG with Existing LLM-Based Methods.

**Prompt: umbrella**

```

<svg xmlns="http://www.w3.org/2000/svg" viewBox="0 0 200 200" width="200" height="200">
<!-- The top of the umbrella -->
<path d="M50,60 Q100,20 150,60" fill="#3498db" stroke="black" stroke-width="2" />
<!-- The pole of the umbrella -->
<rect x="95" y="60" width="10" height="90" fill="#884513" stroke="black" stroke-width="2" />
<!-- The edge of the umbrella -->
<path d="M50,60 Q45,80 55,100 Q100,120 145,100 Q155,80 150,60" fill="rgba(0,0,0,0)" stroke="black" stroke-width="2" />
<!-- The decorative line of the umbrella -->
<line x1="100" y1="60" x2="150" y2="80" stroke="black" stroke-width="2" />
<line x1="100" y1="60" x2="150" y2="80" stroke="black" stroke-width="2" />
<line x1="100" y1="60" x2="70" y2="90" stroke="black" stroke-width="2" />
<line x1="100" y1="60" x2="130" y2="90" stroke="black" stroke-width="2" />
<!-- The ribs of the umbrella -->
<stroke-width="2" />
<!-- The pole of the umbrella -->
<path d="M100 100 Q105 140 110 180" stroke="#000" stroke-width="4" fill="none"/>
<!-- The handle of the umbrella -->
<path d="M110 180 Q120 185 110 190" stroke="#000" stroke-width="4" fill="none"/>
</svg>

```

GPT-o1-preview

```

<svg xmlns="http://www.w3.org/2000/svg" enable-background="new 0 0 128 128" viewBox="0 0 128 128">
<path d="m60.2 96.55-,31-42.82 5.57,31.31 44.83z" fill="#6aa5ad"/>
<path d="m47.46 104.64c-3.27-,16-4.94 2.31-4.52 6.93s3.14 11.63 12.6 11.45c10.92-.21 11.75-7.8 11.57-16.21-.12-5.85 0-10.48-.31-10.69s-7.9-.41-8.32.01-.11 9.56-.21 11.76.28 6.62-3.78 6.51c-3.15-.09-3.57-2.73-3.57-3.99.01-1.25.74-5.56-3.46-5.77z" fill="#3f737f"/>
<path d="m52.12 36.21 10.42-18.75s-20.55-2.54-38.8 11.63c-23.2 18.02-19.53 37.77-19.53 37.77s8.84-8.42 16.07-7.78 16.29 9.39 16.29 9.39z" fill="#937ef3"/>
<path d="m65.06 23.21-1.49-5.75s20.87-.23 36.42 9.96c26.73 17.52 23.78 37.08 23.78 37.08s-5.8-8.08-18.54-7.51-17.4 11.94-17.4 11.94z" fill="#5547f4"/>
<path d="m87.86 68.12s-1.16-19.12-5.6-28.95c-8.1-17.95-19.25-21.42-19.25-21.42s-13.42 6.6-20.48 22.87-5.85 27.76-5.85 27.76 10.86-12.41 26.67-10.7 24.51 10.44 24.51 10.44z" fill="#6e62ed"/>
<path d="m59.11 18.23c-.14-.55-.02-7.9-.07-9.48-.07-2.34 1.92-3.83 3.71-3.78 2.34.07 3.16 2.13 3.23 3.57s.08 9.52.07 9.62c-.09.84-1.32 1.64-3.5 1.65-1.59 0-3.25-.82-3.44-1.58z" fill="#6ca4ab"/>
<path d="m87.79 70.59c1.64-.1 8.19-11.36 18.47-11.26 13.95.14 15.75 7.39 17.21 6.64 1.61-.82-.76-3.83-2.87-6.01-2.98-3.08-7.75-4.94-15.16-4.46-10.79-7.17 10.27-17.75 10.27s-9.2-10.04-25.33-10.04-15.6 0-25.67 11.1-25.67 11.1s-5.1-9.02-17.51-9.24c-10.96-.18-15.7 8.65-14.93 9.42s6.61-6.23 14.8-5.88c11.26.48 15.2 9.89 17.36 9.94 2.15.05 10.56-11.3 26.15-11.03 16.74.29 23.69 10.65 25.23 10.55z" fill="#004dae"/>
</svg>

```

LLM4SVG (Ours)

```

<svg xmlns="http://www.w3.org/2000/svg" viewBox="0 0 200 200" width="200" height="200">
<!-- The surface of the umbrella -->
<path d="M100 100 Q100 20 190 100" fill="#ff6347" stroke="#000" stroke-width="2"/>
<!-- The ribs of the umbrella -->
<path d="M100 100 L10 100 M100 100 L55 60 M100 100 L145 60 M100 100 L190 100" stroke="#000" stroke-width="2"/>
<!-- The pole of the umbrella -->
<path d="M100 100 Q105 140 110 180" stroke="#000" stroke-width="4" fill="none"/>
<!-- The handle of the umbrella -->
<path d="M110 180 Q120 185 110 190" stroke="#000" stroke-width="4" fill="none"/>
</svg>

```

Claude 3.5-pro

Figure S4. Example SVG Code Generated by GPT-o1-preview [2], Claude 3.5-sonnet [35], and Our LLM4SVG.

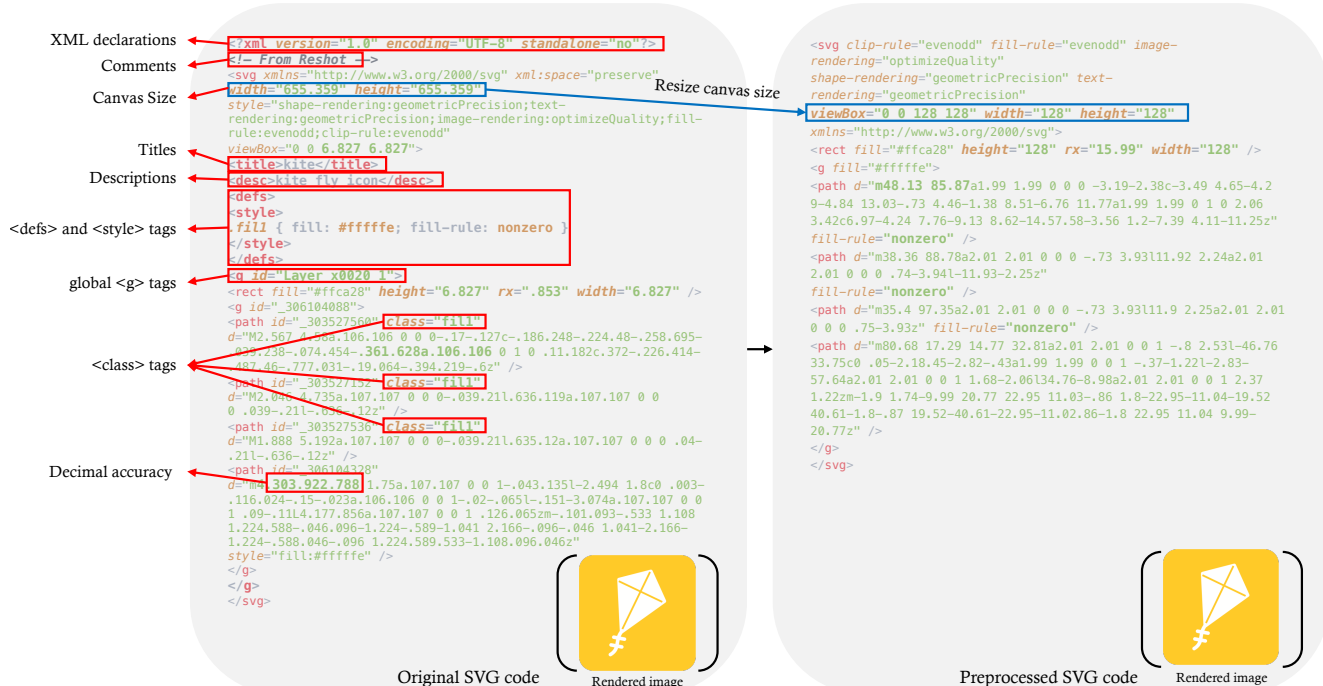


Figure S5. Illustration of our SVG Processing Pipeline.

efficiency. As illustrated in Fig. S5, we remove redundant elements of SVGs, such as XML declarations, comments, titles, descriptions, <def> and <class> tags, and global <g> tags. We also resize the canvas size to 128 × 128, along with adjusting all coordinates of each primitive. Finally, we round decimals to a maximum of two decimal places. These operations preserve the visual output of the SVGs while improving the efficiency of training.

Following the preprocessing of the SVGs, we structured the training instruction template for both SVG generation and understanding tasks. For understanding tasks, we converted all SVGs into raster images and employed GPT-4 [2] to generate detailed descriptions, which serve as the learning content. For generation tasks, we utilized captions generated by BLIP [26] as prompts, with the SVG source code serving as the learning content. In total, our dataset comprises 580k unique high-quality SVG-text instruction-compliant samples.

### C. More Details about User Study

We conducted a user survey to evaluate the effectiveness and practicality of the SVGs generated by our method LLM4SVG and two other popular LLMs, GPT4-o and Claude-3.5. Specifically, the user study was structured as follows:

- Data Preparation:** We randomly sampled 17 text descriptions from the evaluation dataset and generated corresponding SVGs using the three models. Along with

### LLM4SVG user study

There are five SVGs generated based on the given text prompt by some models, please evaluate the five SVGs below based on three dimensions: Prompt Alignment, Visual Quality, and Pick Score.

- Prompt Alignment: How well does this SVG align with the given prompt? (Rated on a scale from 1 to 5, where 1 indicates the lowest score, while 5 represents the highest score.)
- Visual Quality: How appealing is the visual design of this SVG? (Rated on a scale from 1 to 5, where 1 indicates the lowest score, while 5 represents the highest score.)
- Pick Score: Would you consider using this SVG in real-world scenarios? (Yes/No)

\* 01 prompt: "dolphin"



Rated on a scale from 1 to 5, where 1 indicates the lowest score, while 5 represents the highest score.

worst best

Prompt Alignment: How well does this SVG align with the given prompt?

★ ★ ★ ★ ★

Visual Quality: How appealing is the visual design of this SVG?

★ ★ ★ ★ ★

Pick Score: Would you consider using this SVG in real-world scenarios? (Yes/No)

Yes

No

Figure S6. Screenshot of Our Questionnaires.

- the original 17 SVGs from the dataset, this provided a total of 68 SVGs for the user study.
- Questionnaire Design:** Each questionnaire displayed 5 SVGs, randomly sampled from the pool of 68 SVGs.



Figure S7. Additional Results Generated by Our LLM4SVG.

These SVGs were not necessarily generated from the same prompt.

As illustrated in Fig. S6, participants were asked to evaluate each SVG on three aspects:

- **Prompt Alignment:** How well does this SVG align with the given prompt? (Rated on a scale from 1 to 5, where 1 indicates the lowest score, while 5 represents the highest score.)
- **Visual Quality:** How appealing is the visual design of this SVG? (Rated on a scale from 1 to 5, where 1 indicates the lowest score, while 5 represents the highest score.)
- **Pick Score:** Would you consider using this SVG in real-world scenarios? (Yes/No)

3. **Result Calculation:** This user study involves 37 volunteers from backgrounds in computer science and the

arts. Each volunteer was required to complete between 1 and 3 questionnaires. Scores presented in Table 3 of our manuscript were calculated by averaging the ratings for SVGs within the same category. For “Prompt Alignment” and “Visual Quality”, the ratings were adjusted by a coefficient  $\alpha = 0.2$ , such that a score of 1 translates 0.2, and a score of 5 counts to 1. For “Pick Score”, a “Yes” was scored as 1, while a “No” was scored as 0.

#### D. Additional Qualitative Results

In Fig. S7, we present additional results generated by LLM4SVG. These examples demonstrate the model’s capability to produce SVGs that not only maintain semantic integrity but also exhibit high visual quality.